Agricultural and Forest Meteorology 150 (2010) 1245–1257

Contents lists available at ScienceDirect

Agricultural and Forest Meteorology

journal homepage: www.elsevier.com/locate/agrformet

The intense 2007–2009 drought in the Fertile Crescent: Impacts and associated atmospheric circulation

Ricardo M. Trigo[a,b,*], Célia M. Gouveia[a,c], David Barriopedro[a]

[a] IDL, CGUL, Faculdade de Ciências, Universidade de Lisboa, Portugal
[b] Departamento de Engenharias, Universidade Lusófona, Lisbon, Portugal
[c] Escola Superior de Tecnologia, Instituto Politécnico de Setúbal, Setúbal, Portugal

ARTICLE INFO

Article history:
Received 8 March 2010
Received in revised form 10 May 2010
Accepted 14 May 2010

Keywords:
Drought
Fertile Crescent
Precipitation
NDVI
Crop yield
Lake level

ABSTRACT

The historical region of Fertile Crescent (FC) was recently hit by an intense and prolonged drought episode during the two hydrological years spanning between 2007 and 2009. Here, we characterize the temporal and spatial extents of this extreme drought at the monthly and seasonal scales and perform a first assessment on the associated impact in the hydro-meteorological fields, as well as the consequent influence on vegetation dynamics and cereal productions.

This episode corresponds to the driest two-year case for the FC area since 1940, although just slightly drier than the 1998–2000 drought. Precipitation decline was mostly noticeable over Iraq (up to 70%), with the suppression of rainfall particularly acute during the first hydrological year (2007–2008). From the meteorological perspective, winter and transition months were dominated by high pressures that inhibited synoptic activity entering from the eastern Mediterranean and favoured relative north-easterly winds and drier air masses with low convective instability.

The impact of the 2007–2009 drought in vegetation was evaluated with Normalized Difference Vegetation Index (NDVI) obtained from VEGETATION instrument. It is shown that large sectors of south-eastern Turkey, eastern Syria, northern Iraq and western Iran present up to six months of persistently stressed vegetation (negative NDVI anomalies) between January and June 2008. During the following dry year (2008–2009) dry areas are restricted to northern Iraq with up to five months of stressed vegetation. Finally we looked at the impacts on cereal production (wheat and barley) in the region and it is shown that the major grain-growing countries in the area (Syria, Iraq and Iran) were significantly affected by this drought, particularly in the year 2008.

1. Introduction

The historical region of Fertile Crescent area (FC, hereafter) was recently hit by an intense and prolonged drought episode as a consequence of the very low values of precipitation registered during the two hydrological years comprised between 2007 and 2009. This drought event had major socio-economic impacts in several countries located within the affected area, namely; Iraq, Jordan, Syria and Iran. The economic impact was mostly due to the steep decline in agricultural productivity in the highly populated areas of the Euphrates and Tigris river basins (Shean, 2008a,b,c).

The precipitation regime over the FC is characterized by a strong seasonal behaviour, with a rainy season mostly concentrated between November and March. While the average precipitation in transition months (e.g. April, May, October) has a small impact on annual totals, summer (June to September) precipitation can be considered irrelevant. Therefore, all major droughts in this region are characterised by the lack of rainfall during several months of the winter half of the year (e.g. Soltani et al., 2007). The occurrence of droughts in this semi-arid region is a usual feature driven by its precipitation regime, characterised by a strong inter-annual and decadal variability (e.g. Morid et al., 2006; Freiwan and Kadioglu, 2008). Mountainous regions of eastern Turkey and northern Iraq are vital because they induce orographic precipitation that supply the flow of the Euphrates and Tigris rivers, which play a crucial role feeding the Mesopotamia region since the beginning of civilization (Evans et al., 2004) and could decrease dramatically in the future (Kitoh et al., 2008). Furthermore, the movement of pressure systems, such as the incursion of Mediterranean storm track, the convective instability and the upslope flow all can con-

* Corresponding author at: Centro de Geofísica da Universidade de Lisboa, Departamento de Engenharia Geográfica, Geofísica e Energia, Faculdade de Ciências, Univ. de Lisboa, Campo Grande, Ed C8, Piso 6, 1749-016, Lisboa, Portugal.
Tel.: +351 217500855; fax: +351 217500977.
E-mail address: rmtrigo@fc.ul.pt (R.M. Trigo).

0168-1923/$ – see front matter © 2010 Elsevier B.V. All rights reserved.
doi:10.1016/j.agrformet.2010.05.006

tribute to the production of precipitation in the region (Evans et al., 2004).

In this environment, natural vegetation and non-irrigated crops are crucially dependent on soil moisture provided by seasonal rains or springtime snowmelt. This dependence leads to quite different vegetation activity levels on seasonal and inter-annual time scales (Dall'Olmo and Karnieli, 2002; Weiss et al., 2004). Consequently, opportunistic annual species may appear rapidly in response to humid condition of the soil and their greenness is mainly related to recent precipitation (Zaitchik et al., 2007). On the other hand, winter crops and persistent vegetation are dependent on deeper reserves of soil moisture and their vegetative cycle is the result of the combined effect of precipitation (over weeks and months), evaporation and in some regions, of temperature.

The strong dependence of vegetation dynamics on water availability has been for long recognized in the Mediterranean and other semi-arid regions (Eagleson, 2002; Rodríguez-Iturbe and Porporato, 2004; Vicente-Serrano and Heredia-Laclaustra, 2004; Vicente-Serrano, 2007). A combined effect of lack of precipitation over a certain period with other climatic anomalies, such as high temperature, high wind and low relative humidity over a particular area may result in reduced green vegetation cover. When drought conditions end, recovery of vegetation may follow (Nicholson et al., 1998) but such recovery process may last for longer periods of time (Diouf and Lambin, 2001).

Traditional methods of drought assessment and monitoring depend heavily on rainfall data as recorded in meteorological and hydrological networks. However, the recent availability of reliable satellite imagery covering wide regions over long periods of time has progressively strengthen the role of remote sensing in environmental studies, in particular in those related to drought episodes (Kogan, 1995, 1997, 2000; Kogan et al., 2004; McVicar and Jupp, 1999, 2002; Gouveia et al., 2009). Drought early warning systems and monitoring tools are crucial components of drought awareness and mitigation plans (Wilhite, 1993). In fact, it should be stressed that, with the help of environmental satellites, drought episodes can be detected 4–6 weeks earlier than before and delineated more accurately (Kogan, 2000; Gouveia et al., 2009). Over the Middle East area a few satellite drought monitoring applications have been proposed for specific countries such as Iran (e.g. Bajgiran et al., 2008). However to the best of our knowledge none has dealt explicitly with the entire region and covering the outstanding 2007–2009 drought episode. Thus the main objectives of this paper are:

1. To characterize the temporal and spatial extent of this extreme drought event for the two consecutive hydrological drought years of 2007–2008 and 2008–2009 at the monthly and seasonal scales.
2. To evaluate the impacts of this extreme drought episode using appropriate satellite derived information relative to lake levels, agricultural production, and vegetation greenness taking into account different land cover settings.

Data and methodologies employed in this research are presented in Section 2; then, a detailed characterization of the spatial and temporal extent of this drought event and the corresponding anomalous atmospheric circulation are described in Section 3. Section 4 describes the impact of the drought in vegetation dynamics and agricultural production. Finally, the discussion and main conclusions of results are presented in Section 5.

2. Methods

2.1. Precipitation dataset

The monthly precipitation dataset at $1.0^\circ \times 1.0^\circ$ resolution, provided by the GPCC (Rudolf and Schneider, 2005) was used to visualize the spatial extent of the 2007–2009 drought. This dataset, freely available at the GPCC site (http://gpcc.dwd.de), has already been used to analyse extreme dry precipitation episodes over Europe (e.g. Rudolf and Meyer-Christoffer, 2005; Garcia-Herrera et al., 2007). The GPCC database covers the period from 1901 to present through two datasets: the so-called full data product, available for the period 1901–2007 and the monitoring product (version 2) from 2007 to present. The latter is based on quality-controlled data from a station network database available via the Global Telecommunication System (GTS) of the World Meteorological Organization (WMO). The former is optimized for best spatial coverage, although with irregular cover in time, after including non-real-time data from a large number of stations provided by national and regional centres. Therefore, the variable number of stations per grid over time can suffer from inhomogeneity for specific regions. After an exhaustive analysis based on the geomorphology, climatological precipitation regime and availability of GPCC gauge stations over this region, the FC was defined as represented in Fig. 1a. As a consequence, some grid points were excluded from further analysis, namely the coastal regions (Israel and Lebanon) with many more observations since the 1980s. For the selected area, years before the 1940s were scarce in precipitation data (not shown). Therefore, the analyzed period will be confined to the 70-year long period spanning between 1940 and 2009, for which at least 10 stations per month were available. Grid points with at least one gauge station at any time of the analyzed period are indicated with black points in Fig. 1a. Unfortunately, the short record provided by the monitoring product dataset of the GPCC (2007–2009) does not allow performing exhaustive comparative climatologies with the full dataset product (1901–2007). However, a comparison of both datasets for their overlapping year (2007) showed no significant differences over the selected region.

The average precipitation field for the wet part of the year (Oct–May) is shown in Fig. 1b where the large differences between wet and dry regions within the FC region can be appreciated. FC area can be broadly classified as a temperate semi-arid region, with strong north-south precipitation gradient between wet mountainous regime over Turkey and northern Iraq/Iran sector and the much drier area of northern Saudi Arabia and southern Iraq. Equally, there is a strong precipitation gradient on the E–W direction between the Mediterranean coastal mountain ranges and the southern Iraq and northern Saudi Arabia dry sector (Fig. 1b).

A slightly modified version of the standard definition of hydrological year yr–$yr+1$ (i.e. the period spanning between September of year yr to August of year $yr+1$) will be used hereafter, taking into account the concentration of precipitation in the extended winter season. Therefore, our attention will focus on the short version of the hydrological year between October and May in order to concentrate the analysis when it matters and not be distracted by dry months (June–September). As an exception, analyses for the accumulated precipitation during two consecutive hydrological years yr–$yr+2$ will include all the months spanning between October of year yr and May of year $yr+2$.

2.2. Atmospheric circulation variables

The analysis of the atmospheric circulation at the monthly and seasonal scales over the Middle East sector (15°N–60°N lat, 15°E–75°E lon) relies on the NCEP/NCAR reanalysis, available

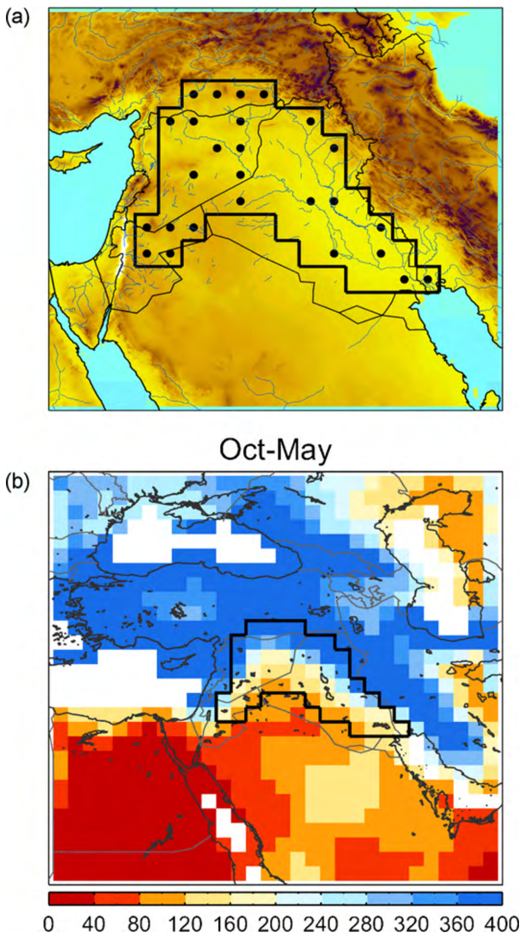

Fig. 1. (a) Middle East region showing the delimited area of the FC (thick solid line) based on 1° × 1° gridded precipitation data from the GPCC. Black dots highlight those grid points within the FC with at least one gauge station available for a given lapse time throughout the 1940–2009 period. Topography and major rivers in the region are also shown; (b) 1940–2009 climatological monthly precipitation (mm) accumulated for the hydrological year (i.e. between October and May). The FC area is highlighted.

since 1948 (Kalnay et al., 1996). Geopotential height, temperature, humidity and zonal and meridional wind components at different pressure levels are provided in a 2.5° × 2.5° regular grid. Furthermore we have retrieved surface variables such as precipitable water. Besides these primary variables we have also computed additional fields with the aim of helping to explain the anomalous precipitation regime during the affected years. As a measure of synoptic activity (storm tracks), the standard deviation of high-pass (2–5 days) geopotential height daily fields at 500 hPa has been computed. The choice of the temporal window was reduced from the typical one adopted in the Mediterranean area (2–7 days), as many of the synoptic disturbances that affect the area have shorter lifetimes. In order to characterise the regional mechanisms capable of inducing precipitation two additional fields have been derived. The first one is the vertically integrated moisture transport through the 1000–500 hPa layer (e.g. Trenberth and Guillemot, 1995). The second choice is related to the convective instability, defined as the equivalent potential temperature difference between 1000 hPa and 500 hPa. The former provides a measure of the water content supply, whereas the latter estimates the atmosphere's tendency for vertical movements.

2.3. Satellite vegetation health index

The response of vegetation to climate forcing was assessed with fields of Normalized Difference Vegetation Index (NDVI), as derived from images acquired by the VEGETATION instrument on-board both SPOT 4 and SPOT 5 satellites. VEGETATION is an optical multi-spectral instrument that performs an almost complete cover of the Earth surface in four spectral bands, on a daily basis (Hagolle et al., 2005). NDVI data were extracted from the so-called S10 products of the VITO database (http://free.vgt.vito.be), which are supplied at the resolution of 0.008928° (i.e. about 1 km^2 resolution at the equator) in geographic coordinates (Lat/Lon). We have restricted the analysis to the region extending from 25°N to 48°N and from 33°E to 56°E and to the period that spans from September 1998 to August 2009.

NDVI values were derived from atmospherically corrected and geometrically calibrated data. Details on the corrections methods can be found in Maisongrande et al. (2004). NDVI fields from VITO are provided on a 10-day basis as derived using the Maximum Value Composite method (MVC), which selects, for each pixel, the date of maximum NDVI among 10 consecutive daily images (Holben, 1986). Time series of MVC-NDVI composites have proven to be a source of valuable information for monitoring surface vegetation dynamics at the global and the regional scales (Zhou et al., 2001; Lucht et al., 2002; Nemani et al., 2003). It is worth stressing that choice of VGT-NDVI in detriment of longer NDVI datasets (e.g. based on NOAA-AVHRR data) was motivated by the higher resolution provided by the VEGETATION instrument which allows a proper quantification of the land cover types associated to each drought event.

2.4. Satellite surface water level

Water level time series for Lake Tharthar (Iraq) were obtained with satellite radar altimetry from 3 consecutive satellite platforms (Topex/Poseidon, Jason-1 and Jason-2). The Jason-2 or Ocean Surface Topography Mission (OSTM) was launched on June 20, 2008. It is the follow-on satellite to the Topex/Poseidon (1992–2002) and Jason-1 (2002–2008) missions, and continues the observations of surface water levels. A satellite radar altimeter is not an imaging device, but a nadir-pointing instrument continuously recording average surface 'spot' heights directly below the satellite, as it transverses over the Earth's surface. Operating at ~13.6 GHz, each altimeter emits a series of microwave pulses towards the surface. By noting the two-way time delay between pulse emission and echo reception, the surface height can be deduced. Each returned height value is an average of all surface heights found within the footprint of the altimeter. Each satellite is placed in a specific repeat orbit, so after a certain number of days the same point (to within 1 km), on the Earth's surface is revisited. In this way, time series of surface height changes can be constructed for a particular location along the satellite ground track during the lifetime of the mission.

Although their primary objectives are ocean and ice studies, altimeters have had considerable success in monitoring inland water bodies. In particular, the ability to remotely detect water surface level changes in lakes and inland seas has been demonstrated (Chen et al., 2001; Cretaux et al., 2005). Unhindered by time of day, weather, vegetation or canopy cover, the technique has further been applied to a number of rivers, wetlands and floodplains in several test-case studies. Results demonstrate how submonthly, seasonal, and inter-annual variations in height can be monitored.

Sensor and water surface level dataset characteristics are given in detail in the USDA site (http://www.pecad.fas.usda.gov/cropexplorer/global_reservoir/index.cfm). As several correction fields are still being finalized, the raw height time series should be used carefully. Here we have used the smoothed version obtained

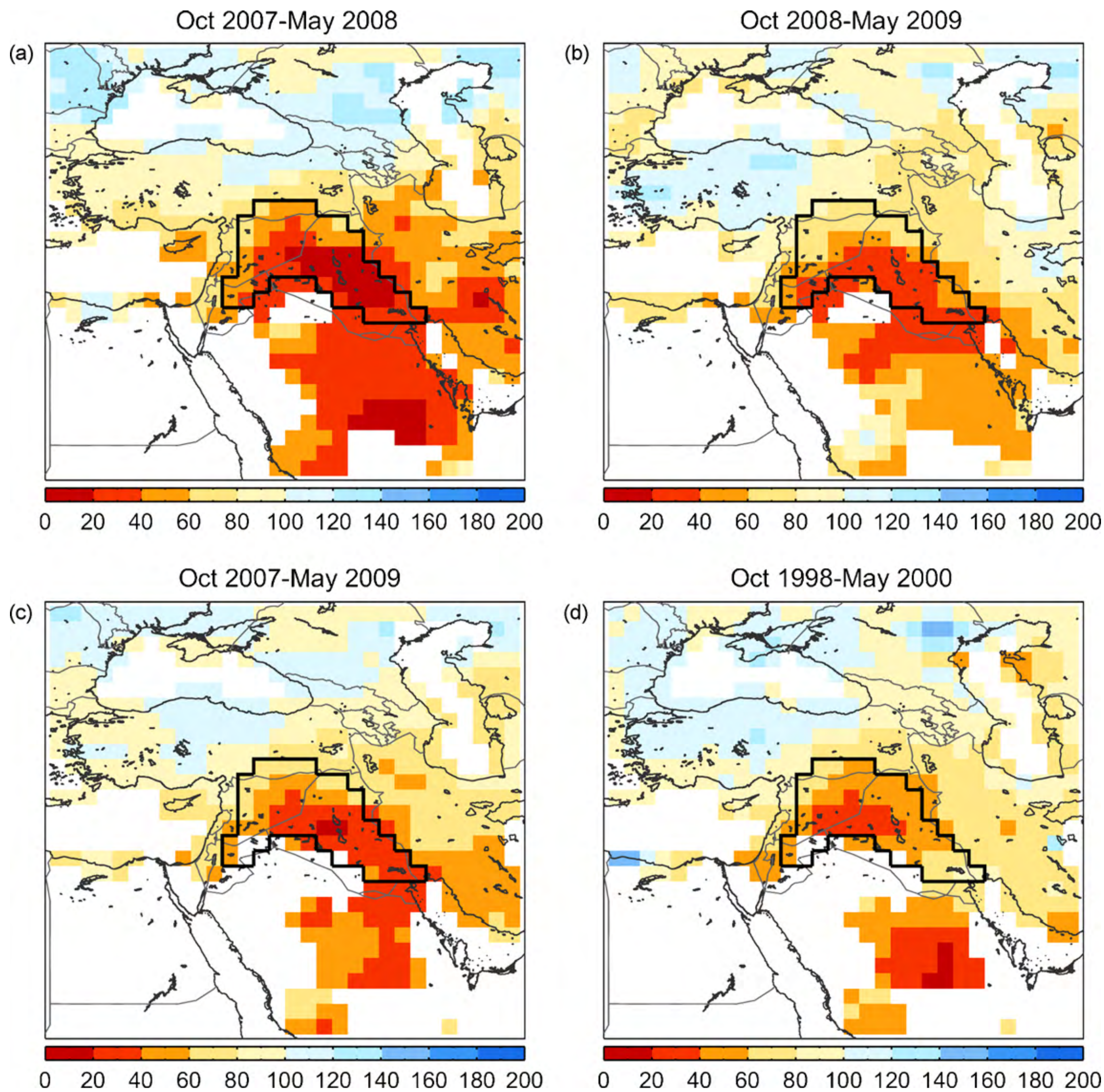

Fig. 2. Accumulated monthly precipitation (expressed in percentage relative to the 1940–2009 normals) during the hydrological years: (a) 2007–2008; (b) 2008–2009; (c) 2007–2009; (d) 1998–2000. Only grid points with climatological accumulated precipitation above $N \times 10$ mm are shown, where N is the number of months considered in each case (8 months in a and b and 20 months in c and d).

after applying a median type filter to eliminate outliers and reduce high frequency noise.

All monthly anomaly fields computed in this work were obtained after removing the corresponding climatological normals for the total available period, which comprise 1940–2009 for precipitation and 1948–2009 period for the rest of atmospheric data. However, monthly NVDI anomalies are defined as departures from the median of that month (computed over the full available period 1998–2009). The median (instead of the mean) was employed in order to avoid the distorting effect caused by the extremely low NDVI values that were attained during droughts years, taking into account the small length of the sample (12 years).

3. Results and discussion

3.1. Spatial and temporal characteristics of the drought

3.1.1. Spatial context

As stated in Section 1, precipitation in the Middle East is almost entirely observable between October and May (Fig. 1b), unusual dry (wet) years being always characterised by less (more) than normal precipitation during that core period. Therefore, to assess the drought episode the accumulated precipitation percentages for the hydrological year have been computed with respect to the corresponding climatological (1940–2009) normals (Fig. 2). This evaluation was done over the entire Middle East area, between October 2007 and May 2008 (Fig. 2a), and between October 2008 and May 2009 (Fig. 2b). In order to avoid misleading results over dry areas the percentage anomalies shown were restricted to those areas with climatological monthly mean rainfall amounts above 10 mm/month (i.e. climatological accumulated precipitation above 80 mm for the October–May period).

It is immediately striking the intense decline in precipitation during both years over the FC area, although this decline is not confined to the FC region. The vast geographical area struck by this intense drought episode extended from Israel (west) to Iran (east) and Saudi Arabia Peninsula but was particularly severe over the Iraq, Kuwait and northern Saudi Arabia territories. This decline is stronger in the first hydrological year, surpassing 80% less rainfall over central Iraq (Fig. 2a), and of the order of 70% less in the second hydrological year (Fig. 2b). If we aggregate the two consecutive hydrological years the emerging pattern falls in between, with several grid points over Iraq characterised by extremely low values of

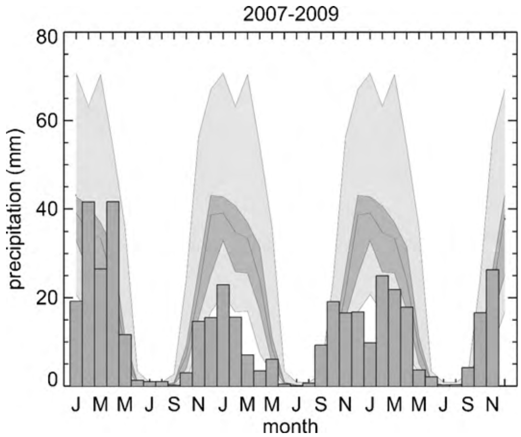

Fig. 3. Time series of the monthly precipitation averaged over the FC area for the 2007–2009 period (grey bars). Dark (light) shaded curve comprises the 30th–70th (10th–90th) monthly percentiles with the median in between (solid line) obtained from the 1940–2009 precipitation time series.

precipitation and most of the FC area recording precipitation values that were below 40% of its climatological normal (Fig. 2c). For the sake of comparison, we also present the corresponding pattern relative to the previous major 2-year drought that took place between 1998 and 2000 (Fig. 2d), which was somewhat similar, although not as intense in several grid points.

3.1.2. Temporal evolution

Besides the relatively widespread impact of this drought, its temporal evolution over the years 2007–2009 deserves a more in depth analysis. For this purpose we have averaged the precipitation for the FC area previously defined (Fig. 1a) and the obtained time series between January 2007 and December 2009 can be seen in Fig. 3. In order to put these values into a longer context we also present the climatological median and the 10th, 30th, 70th and 90th percentile curves, all computed with the entire 70-year period (1940–2009). Looking at each year it can be noted that the winter–spring period of 2007 was relatively wet, with at least two months (February and April) standing above the 70th percentile. This is relevant because it helped to damp the first dry months of the subsequent hydrological year. In fact, the two following hydrological years are almost always below the average during the wettest months, particularly between October 2007 and May 2008. However, this annual evolution was relatively distinct as during the 2007–2008 hydrological year every month presented values below the 10th percentile of the long-term climatology (except January). On the contrary, the second drought year starts with a relatively wet autumn (SON) period (in accordance to Fig. 2b) followed by an extremely dry winter, with values below or close to the 10th percentile, while spring 2009 although dry was not comparable with the previous spring 2008.

It is worth noticing the double-year nature of this drought, where the effects of the drought on the second hydrological year (2008–2009) were enhanced by the magnitude of the previous outstanding drought year (2007–2008). This fact is particularly relevant for water resources management, as it highlights the water-stressed level already present at the beginning of the 2008–2009 hydrological year. Naturally, despite the observed wet October 2008, levels of soil moisture decreased continuously since the end of 2007, reaching extremely low values at the end of spring 2009 with negative impacts on vegetation growth, as it will be shown in Section 4.

With the aim of evaluating the rank of this prolonged drought event we have computed the accumulated monthly precipitation (averaged over the FC area) for the two consecutive hydrological years, i.e. between October 2007 and May 2009 (Fig. 4). The corresponding evolution of the associated climatological accumulated monthly precipitation distribution for the FC region is also

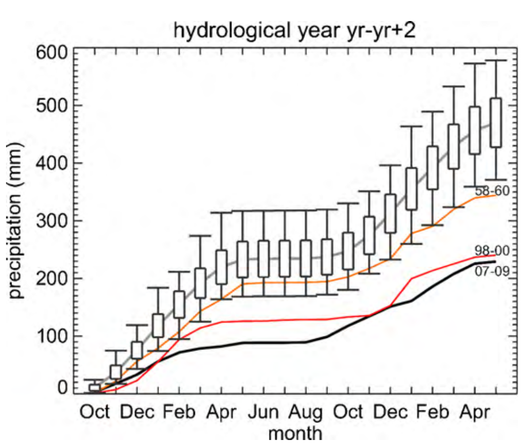

Fig. 4. Accumulated monthly precipitation averaged over the FC area during two consecutive hydrological years (from October *yr* to May *yr* + 2). Grey line indicates the climatological mean evolution, with boxes (whiskers) representing the ±0.5 sigma level (10th–90th percentiles) obtained from all consequtive pairs of hidrological years between 1940 and 2009. Black line shows the corresponding evolution for the 2007–2009 drought event. For the sake of comparison the two consequtive most severe drought events within the 1940–2009 period are also indicated.

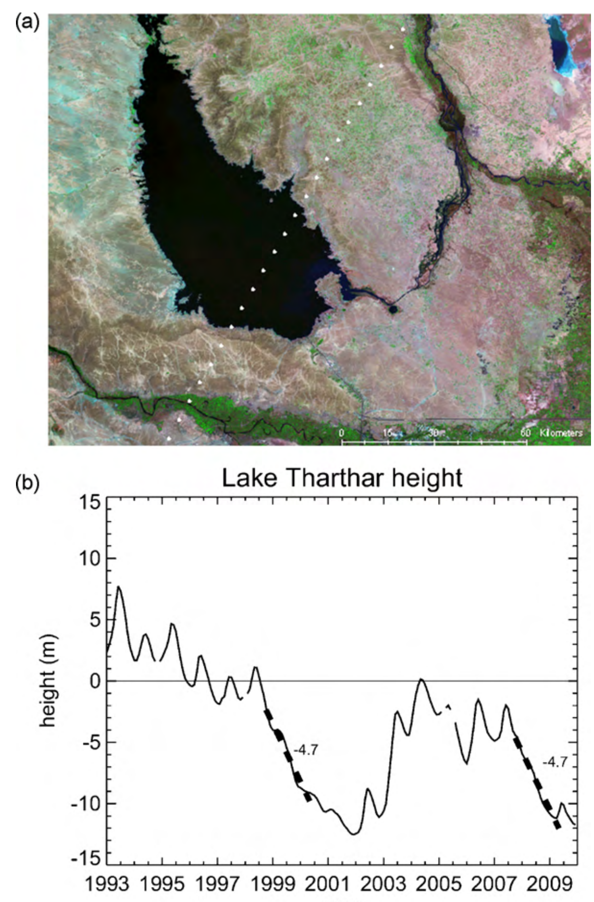

Fig. 5. (a) Satellite image taken in 1990 by Landsat 5 of the Tharthar lake with the orbital path depicted by white dots (figure obtained from USDA site http://www.pecad.fas.usda.gov/cropexplorer/global_reservoir/index.cfm); (b) series of the relative lake height for the 1993–2009 period (in m). Black line indicates the monthly mean values. Thick straight lines represent the linear fit from the monthly values of the two successive hydrological years (October *yr*–May *yr* + 2) for the 1998–2000 and 2007–2009 droughts. The slopes are shown in m/yr.

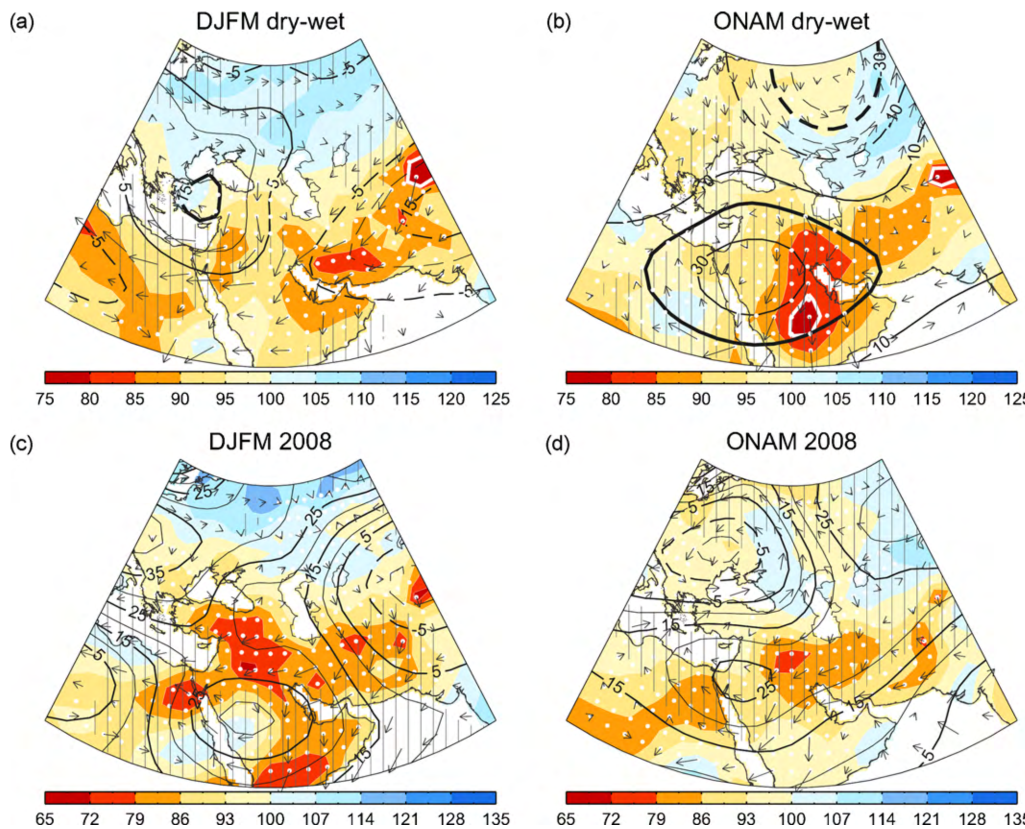

Fig. 6. Seasonal composites of geopotential height at 500 hPa (lines), precipitable water (shaded) and 1000–500 hPa vertically integrated moisture transport (arrows) for: (a) the five driest minus the five wettest DJFM years of the 1948–2006 period over the FC area; (b) as (a) but for ONAM; (c) DFJM 2008; (d) ONAM 2008. Seasonal composites in (c) and (d) are shown as anomalies relative to the 1948–2009 period. Precipitable water is expressed in percentage of normal values. Negative values of the 2–5 days high-pass geopotential height standard deviation and convective instability are marked as vertical grey lines and white dots, respectively. Statistical significant differences at $p < 0.1$ in (a) and (b) are indicated by thick contours.

shown using a standard whiskers plot. As expected, the deficit grows steadily during the winter and spring months of both hydrological years and presents a flat plateau during the summer months (similar to the climatological average). At the end of the considered period (May 2009) the accumulated precipitation (~230 mm) is less than half of the mean value (about 470 mm), corresponding to the lowest accumulated value in two consecutive hydrological years since at least 1940. The second and third most important drought events in two consecutive hydrological years are also represented in Fig. 4, corresponding to the 1998–2000 (red) and the 1958–1960 (orange) events.

3.1.3. Lake level

Lake Tharthar is the largest lake in Iraq with an area of 2710 km^2 and is located 120 km north of Baghdad, between the Tigris and Euphrates rivers. The actual size of the lake varies between winter and summer due to the highly seasonal precipitation (rainfall and snow) regime affecting the mountainous heads of both Middle East rivers in Turkey. Moreover, the inter-annual (and longer term) variability of the lake level can vary as a function of the dry-wet nature of each hydrological year. Lake Tharthar configuration can be seen in Fig. 5a as obtained in 1990 with Landsat 5. The orbital path of the Jason-1 satellite is shown in this image, depicted by series of white points.

The intra-seasonal and inter-annual variability of relative height variations in lake Tharthar between early 1993 and late 2009 are represented in Fig. 5b. This time series was obtained after aggregating data from TOPEX/POSEIDON (T/P) and Jason-1 and Jason-2 altimetry with respect to a 10-year mean level derived from T/P altimeter observations. One can notice the intense seasonal character with peak (dip) lake level observed at the end of spring (autumn) as a consequence of spring snow melt (the lack of precipitation and others water supplies during the central months of the year). Moreover, the existence of a few dams upstream of both Tigris and Euphrates rivers will smooth eventual shorter frequency events and introduce a delay on water flow arriving to lake Tharthar (Jones et al., 2008). However, the most prominent features in this figure are indisputably the two prolonged negative trends in the lake's level, the first spanning between 1998 and 2001 and the second having started in 2007 and still going at the end of 2009, with water levels as low as those reached in 2002. The wet years of 2002–2004 allowed a noticeable recover in the water levels but still considerably lower than those observed in the early 1990s.

3.1.4. Atmospheric circulation

This section aims at providing some highlights on the large-scale features that characterized the drought years of 2007–2008 and 2008–2009 over Iraq. As explained before, the complexity of the area determines different precipitation processes, most of them involving Mediterranean storm tracks, convective precipitation and orographic rainfall (e.g. Evans et al., 2004). In particular, orographic precipitation appears to be of prime importance windward of the mountain chains surrounding the area (the Zagros Mountains to the north-east and the Taurus mountains to the north), where local terrain influences induce considerable higher values of precipitation than at leeward sites.

Over the FC area, precipitation is mainly associated with storm tracks approaching from the Mediterranean or strong convective instability with water vapor supply. The former is the dominant process during most of the winter (from December to March)

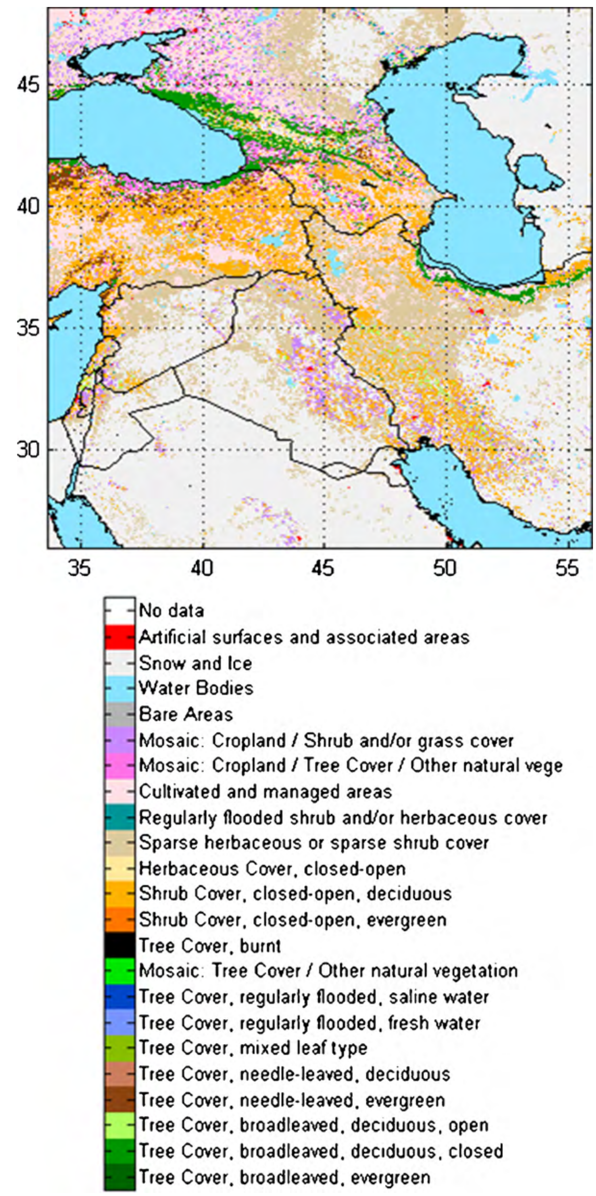

Fig. 7. Land cover classification for the study area as obtained from the Global Land Cover 2000 (GLC2000) database (http://www-gvm.jrc.it/glc2000).

and affect the region through two main paths: south of Turkey into the Caspian Sea and Jordan–Syria into the Persian Gulf (Trigo et al., 1999). In spite of the relative frequency of migratory systems (each 3–5 days), precipitation occurs with associated surface frontal activity, which only accompanies the strongest lows. In particular, Cyprus lows produce more rain in this region than any other type (e.g. Black sea and Atlas lows). As the season progresses into spring, low systems move farther north until they no longer affect the area (Trigo et al., 1999).

A secondary type of precipitation, observed through most of the year, is related to waves or secondary troughs travelling along the subtropical jet stream (STJ) and crossing northern Saudi Arabia. Although they do not usually have surface fronts, south-easterly onshore flows ahead of these systems allow moist, warm Persian Gulf air to move inland, causing isolated thundershowers over the Tigris–Euphrates valley. Sporadically, other local moisture sources, mainly the lakes in the center of Iraq can produce rainshowers. In summer months this process does not usually produce measurable precipitation since the high temperatures evaporate raindrops before they reach the ground.

It should be noted that most of the monthly precipitation is usually associated to a few single precipitating events, even in winter. Therefore, a single rainfall event may determine the monthly precipitation totals and its associated circulation signal could be masked at monthly or seasonal time scales. Thus, before charactering the large-scale features that characterized this drought episode, seasonal composite differences between the five driest and wettest years over the FC area have been computed in order to assess whether the anomalous precipitation have associated circulation signatures at seasonal scales. This diagnostic assessment also provides an estimate of the relative contribution of individual precipitation processes mentioned above, allowing for a better contextualization on the atmospheric circulation associated with the recent drought. The composite fields have been derived separately for the wet (December–March, DJFM) and the transitional months (October–November–April–May, ONAM) of the hydrological year using data between 1948 and 2006, i.e. excluding any data from the 2007–2009 drought episode. The analyzed variables include those described in the Section 2.

Results obtained with the composite differences for winter (DJFM) and transition months (ONAM) are shown in a compact format in Fig. 6a and b, respectively. The circulation anomaly pattern in winter (transition) season reflects a zonal (meridional) height dipole with higher-than-normal pressures centred over Turkey and eastern Mediterranean (contours). As a consequence, winter synoptic transient activity during dry years is reduced over the main Mediterranean cyclogenesis regions (vertical grey lines), including the Mediterranean coastal sector but equally Jordan, Syria and to a less extent Iraq. In transition months, the high pressure signature also reflects weaker synoptic activity but it is placed further south than in winter (including Iraq and the entire Arabian Peninsula), which is suggestive of a reduced activity of the second type of precipitation process (i.e. synoptic waves travelling along the STJ). This is supported by the associated moisture fluxes, which are also different between seasons, as shown by the arrows. In wet winters, the moisture flux reaching the FC area arrives essentially from the eastern Mediterranean and then turns northward and backs to Europe, thus picturing a dominant cyclonic circulation. In wet transition months, water vapor fluxes are supplied by the Persian Gulf and south-easterly winds affect the FC. All these low-level humidity fluxes are suppressed in dry years and hence, the potential for convection is also reduced, as indicated by anomalous negative values of CI (white dots). To a certain extent all these processes seem to contribute to a significant reduction of the PW content during dry years (shaded areas).

It should be stressed that some of the anomaly patterns are only locally significant, which, in addition to the low sample size, seems to support the importance of monthly and submonthly processes. Nevertheless, seasonal composites highlight appreciable signatures and seasonal differences in the mechanisms conductive to precipitation.

Regarding the seasonal composites of the 2007–2009 drought episodes, they reveal a diversity of patterns, but all of them unfavourable for the precipitation mechanisms described before. For the sake of simplicity, we restrict the analysis to a few seasons corresponding to the hydrological year 2007–2008, i.e. the driest one, as shown here (Fig. 6c and d). Vast sectors with high pressures tended to dominate the lower troposphere over large areas spreading through the Middle East and north of it, whereas surface temperatures where above (below) average in transition (winter) months (not shown). Synoptic activity was also weaker than average over the key surrounding areas associated with precipitation in FC, namely, eastern Mediterranean and the latitudinal band encompassing Egypt and northern Saudi Arabia. During both

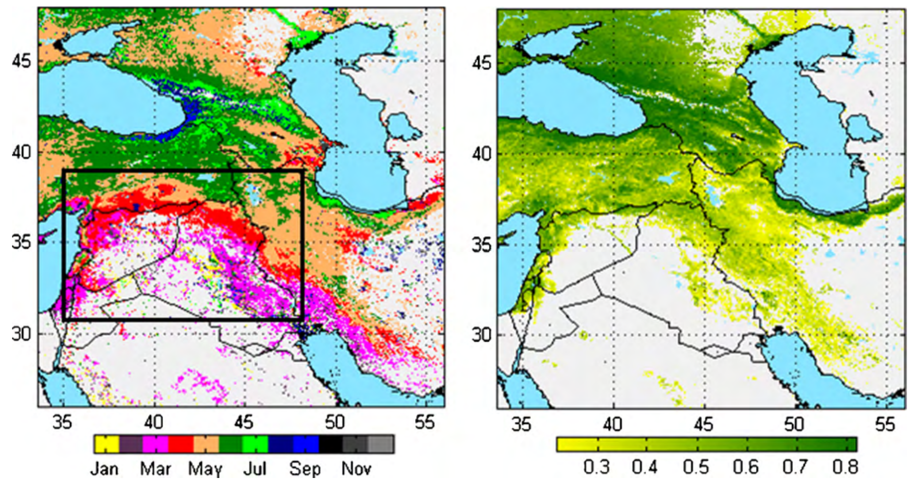

Fig. 8. Spatial distribution of the month with maximum annual mean NDVI, as obtained from monthly average SPOT-VEGETATION data (left panel) and the maximum vegetation greenness, as represented by the NDVI value for the monthly maximum obtained in the left panel (right panel).

seasons, moisture fluxes over the affected area had a relative easterly or north-easterly component as compare to the climatology, and hence, dry advection fluxes from Iran and Russia were frequent, leading to significant reductions in the PW content. The occurrence of relative easterly or north-easterly winds is typical of high pressures over Turkey and the Caspian Sea (clearly observed through most of the hydrological year), which bring dust-free dry air masses into the area. The dry conditions also favoured low

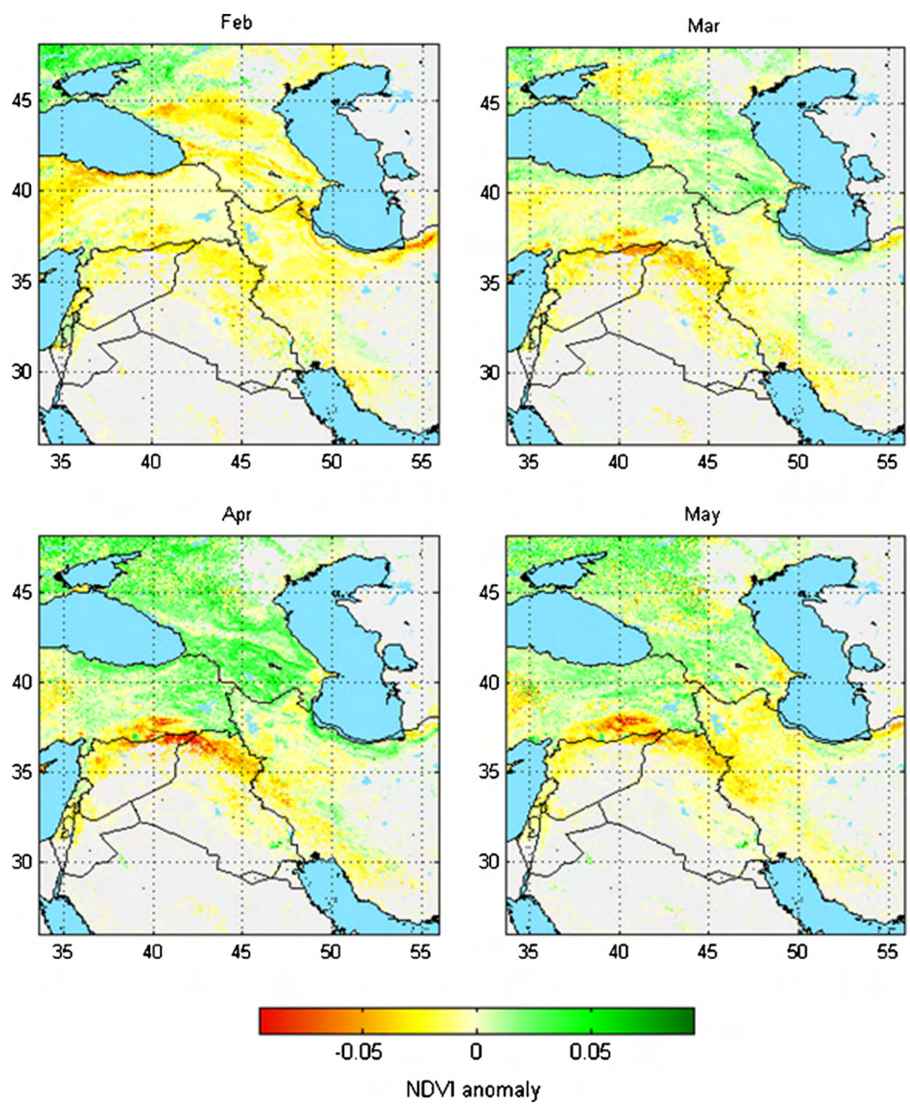

Fig. 9. NDVI anomalies from February to May of the 2007–2008 hydrological year.

potential equivalent temperatures at 1000 hPa and a weaker-than-normal convective instability. These signatures are in agreement with the typical ingredients associated to drought episodes in the FC (Fig. 6a and b). Some differences emerge, though. For instance, the outstanding displacement of the high pressure system into central Saudi Arabia may have contributed to the exceptional seasonal drought (DJFM 2008 was a record-breaking low value).

4. Drought impact on vegetation

4.1. Vegetation dynamics

The land cover types reflect the precipitation regime in the area, characterized by the aforementioned meridional precipitation gradients (Fig. 1b). Information about the land cover type associated to each pixel is also provided (Fig. 7), as obtained from the Global Land Cover 2000 (GLC2000) database (http://www-gvm.jrc.it/glc2000). The main land cover types correspond to the forest and agriculture cover types in the north (between the Caspian and Black seas) and the crops, grassland–shrubland and desert in the FC region. Non-irrigated crops planted in the dry inland areas are particularly sensitive to the significant inter-annual precipitation variability that affects the area, becoming a key factor on crop yields and productivity (Schmidt and Karnieli, 2000; Weiss et al., 2001). In order to assess the impact of drought conditions upon the FC vegetation dynamics it must be noted that the annual cycle of vegetative cycle peaks at different times of the year depending on the land cover type. This seasonal dependence is shown in Fig. 8 (left panel), where we present the spatial distribution of the month corresponding to the maximum of the annual NDVI cycle as derived from monthly average SPOT-VEGETATION data. Pixels corresponding to bare soil, according to GLC2000 classification (Fig. 7) have been masked and represented in light gray.

In order to concentrate the analysis of the drought impact on vegetation we will restrict the assessment to the box represented in Fig. 8 (left panel) that corresponds broadly to the FC region. Therefore, a combined analysis of Figs. 7 and 8 shows that agriculture fields in the northern region correspond to late spring and summer cultures (southern Turkey), while those located further south are mostly winter and early spring crops (notably in northern Syria and Iraq). Additionally, one must take into account the phenology and density of vegetation associated to the monthly peak value as represented by the NDVI value (Fig. 8, right panel). Forests in the mountains of Turkey are characterized by high NDVI values, with vegetation intensity peaking in early summer. The agricultural patterns in the FC (grossly represented by the box in Fig. 8, left panel) are quite different, being limited by summertime dryness rather than wintertime frost.

Our results on land cover greenness sensitivity are in good agreement with those from Zaitchik et al. (2007). These authors have shown that the inter-annual variability in vegetation is larger along the southern edge of the Fertile Crescent, represented in red in Fig. 8 (left panel), with grain crops and forage material growing up in the wet years but disappearing completely in a drought year. They have also analyzed the nature of climate-driven variability using AVHRR data in conjunction with meteorological fields (precipitation and temperature) for different seasons. They have found that NDVI for the FC region is mostly dependent on the winter precipitation, although the northern Iran is also dependent on wintertime temperatures.

4.2. Spatial assessment

The evolution of monthly anomaly fields of NDVI should focus in months characterized by higher photosynthetic activity within

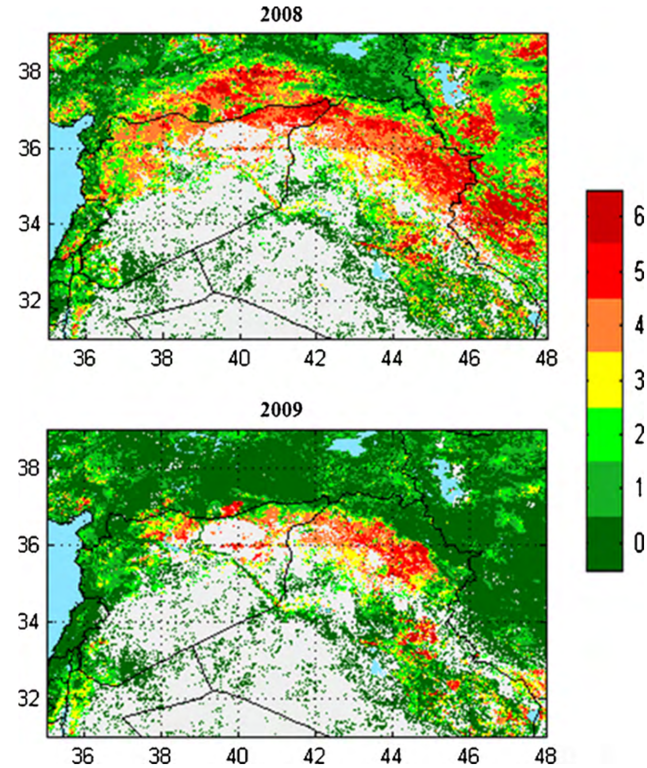

Fig. 10. Number of months between January and June with NDVI anomaly values below −0.010, for 2008 (top) and 2009 (bottom).

the FC area, i.e. from February to May (Fig. 9). The highest negative anomalies (around −0.10) are found in April 2008 and remain with slightly low values and in a small region in May. The most affected region corresponds broadly to the northern FC sector, being less intense over the Mediterranean mountainous area and the Tigris and Euphrates basin in Iraq. It should be noticed that the heads of both Tigris and Euphrates received a relative good amount of water (see Fig. 2) partially offsetting the meteorological dryness over Iraq regions lying along their course. Finally, it is worth stressing that the observed negative NDVI anomalies are contemporaneous with the period of high photosynthetic activity, leading to a further amplification of the negative impact on vegetation dynamics and therefore to an even larger drought impact.

Based on the methodology previously developed by Gouveia et al. (2009) for western Iberia we have also evaluated drought persistence by simply counting, for each pixel, the number of months within the hydrological year with NDVI anomalies lower than a predefined threshold (Fig. 10). The referred methodology should be adapted to different regional settings. Therefore, taking into account the low range of NDVI anomalies we have set the threshold to −0.01, appreciably lower than the −0.025 considered over Iberia. On the other hand, the annual cycle of vegetation dynamics is roughly three months offset from the precipitation cycle and hence, the hydrological year definition does not apply here. Thus, instead of eight months (from October to May), we have only considered a maximum accumulation of up to six months (from January to June), which encloses those months with relevant vegetation activity (Fig. 8, left panel). As for the case of the hydrological year, the period with negative NDVI anomalies is also smaller than that obtained for western Iberia (from September to August, Gouveia et al., 2009).

In the case of the 2007–2008 drought year, pixels located over south-eastern Turkey, eastern Syria, northern Iraq and western Iran reveal up to six months of persistently stressed vegetation, i.e. between January and June 2008 (Fig. 10, upper panel). When we

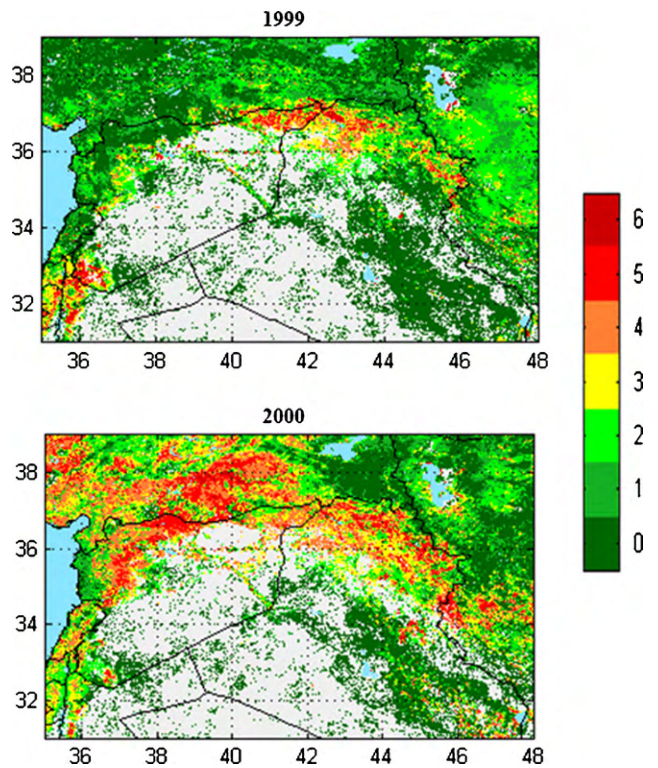

Fig. 11. As in Fig. 9, but for 1999 (top) and 2000 (bottom).

consider the 2008–2009 drought year, the most affected region is smaller, being restricted to northern Iraq, although still revealing a considerable area with up to five months of stressed vegetation (Fig. 10, lower panel).

In order to provide an objective comparison with previous major drought events we have applied the same methodology to the drought years of 1998–1999 and 1999–2000 (Fig. 11), which correspond to the second driest prolonged event in record (see Fig. 4). Generally, the cumulative impact was one month shorter than the one observed for 2007–2008. Nevertheless, the intensity and spatial extent of this prolonged drought event was similar to that displayed by the recent episode. In the case of the 1998–1999 drought year, pixels located over north-eastern and south-western Syria, north Iraq, Jordan and Israel reveal up to five months of persistently stressed vegetation between January and June, this pattern exhibiting some resemblance to the hydrological year 2008–2009. However, in the case of the following 1999–2000 drought year, a much vaster region is under prolonged vegetative stress (up to five months), spreading from northern Syria and Iraq to southern Turkey.

4.3. Land cover sensitivity

We have also compared the vegetation response to water stress relative to different land cover types, for the two major drought episodes of 1998–2000 and 2007–2009 (Table 1). The analysis is confined to pixels located inside the square box represented in Fig. 8 (left panel) that were affected by drought (i.e. those pixels with at least five out of six months of negative NDVI anomalies for the January–June period, Fig. 9). The use of percentages allows a more straightforward comparison between relative affected areas associated with each land cover. However, one should be aware on the larger extension of affected area during the years 2000 and 2008 as given by the total number of affected pixels (Table 1, last row). For all drought years, sparse vegetation represents more than half of all pixels, with the exception of 2000 (44%). The highest percentage of sparse vegetation affected by prolonged drought can be found in 2009 with almost 70% of the affected pixels belonging to this cover type. The following two most represented land cover types are shrub and cultivated-managed areas, with values of affected area between 10% and 20%, except for the year 2000 when both land covers contribute with more than 20% each. The fourth vegetation type corresponds to the mosaic of crops/shrub/grass with percentages lower than 10% and the exception of 1999 (14%).

The cumulative effect of drought conditions on the four types of vegetation was further analysed on the basis of the relative proportion of pixels of each vegetation type that remained negative (NDVI anomalies below −0.010) for three to five months. Results are presented in Table 2 and important differences may be found among the two-year drought episodes. Focusing on the percentage of pixels affected for at least five months, the mosaic crop/shrub/grass was clearly the most stressed vegetation type in 1999 (35%), whereas in the case of the 2000 drought year, 47% of cultivated-managed area suffered from the dry conditions. The exceptional impact of the 2008 drought year on sparse vegetation is well illustrated by the fact that more than half of the pixels are affected for at least five months. The remaining vegetation types considered are also affected for at least five months over circa 40% of pixels. During the 2009 drought year, sparse vegetation was again the most affected land cover type, with around 40% of the pixels being affected. Therefore, whereas the 1998–2000 event impacted on different types of vegetation types, sparse vegetation was severely struck in two consecutive years during the 2007–2009 episode, thus increasing the negative effects of this prolonged drought.

Table 1
Relative proportions and total amounts of pixels affected by drought (for at least five months) for different land cover types and relative to year 1999, 2000 and also 2008, 2009.

	1999	2000	2008	2009
Shrub	0.12	0.22	0.16	0.11
Sparse	0.55	0.44	0.56	0.69
Cultivated	0.16	0.26	0.20	0.09
Mosaic	0.14	0.05	0.07	0.10
Other	0.02	0.03	0.01	0.01
Total	1.00 (42,553)	1.00 (192,303)	1.00 (206,944)	1.00 (63,319)

Table 2
Cumulative effect of drought conditions for specific land covers types during the drought year 1999, 2000 and also 2008, 2009.

	Total	≥3	≥4	≥5
1999				
Shrub	44,723	100%	31%	12%
Sparse	116,989	100%	46%	20%
Cultivated	58,583	100%	33%	12%
Mosaic	16,805	100%	69%	35%
2000				
Shrub	101,199	100%	71%	42%
Sparse	193,364	100%	72%	43%
Cultivated	104,892	100%	70%	47%
Mosaic	29,533	100%	70%	35%
2008				
Shrub	86,402	100%	64%	39%
Sparse	219,182	100%	77%	53%
Cultivated	100,022	100%	64%	41%
Mosaic	32,182	100%	73%	44%
2009				
Shrub	26,608	100%	53%	26%
Sparse	108,512	100%	69%	40%
Cultivated	24,856	100%	45%	23%
Mosaic	19,517	100%	63%	34%

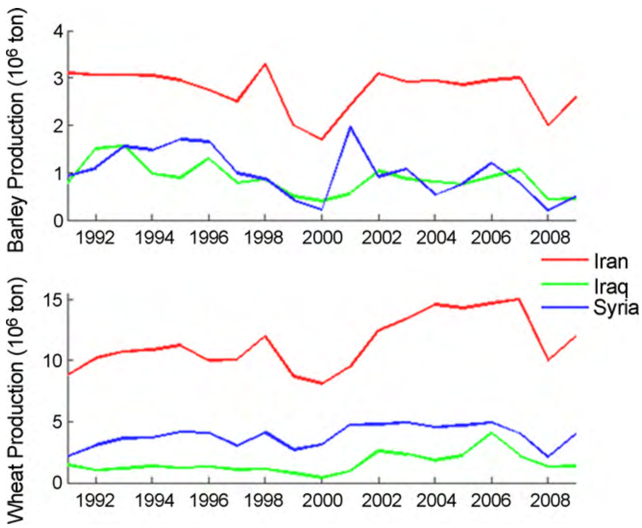

Fig. 12. Inter-annual variability of cereal production between 1980 and 2009 for wheat (bottom panel) and barley (top panel) productions. Time series relative to Iran (red), Iraq (green) and Syria (blue) are represented. Production values obtained from the FAO site (http://faostat.fao.org) (For interpretation of the references to color in this figure legend, the reader is referred to the web version of the article.).

4.4. *Cereal production*

Drought analysis in semi-arid regions is especially important, because they tend to induce large economic losses (Morales et al., 2000; Iglesias et al., 2003), mostly associated to the strong dependence of the regional economy and society on agriculture production (Vicente-Serrano, 2006). As explained above, the most affected regions by the drought are eastern Syria and northern Iraq and Iran, which correspond to the major grain-growing areas of these countries. With the exception of the irrigated areas within the Euphrates and Tigris basin, the vast majority of crops in these regions are non-irrigated and thus dependent on winter precipitation. Dry conditions during the plantation period cause crops failure due to lack of water during the germination of the seeds.

Inter-annual variability of cereal production is depicted in Fig. 12 with wheat (bottom panel) and barley (top panel) productions for Iran (red), Iraq (green) and Syria (blue) from 1980 to 2009. Values of annual production were obtained from the appropriate FAO site, i.e. FAOSTAT (http://faostat.fao.org). The impact of drought is clearly visible during the years 2000 and 2008 in both wheat and barley productions, with significant socio-economic losses in the affected countries (Shean, 2008a,b,c). The exceptionality of the 1999–2000 and 2008–2009 drought events is once again evident with larger than usual dips in production curves during these two-year events. These declines are obviously associated with both the extension and persistence of the drought, and the fact that both prolonged droughts affected vast amounts of cultivated area, including those responsible for the most relevant cereal productions in the FC (wheat and barley). When the whole two-year events are considered, the agricultural impacts of the 2007–2009 drought emerges especially severe in Iraq compared to the 1999–2000 drought, and more acute in barley production, whereas Syria and Iran production levels remained similar or even higher than those for the 1998–2000 drought. As most of the cultivated land cover within the FC box of Fig. 8 belongs to the Iraq territory (Fig. 7), it can be concluded that the 2007–2009 drought event was similar but relatively more harmful in cereal production than the 1998–2000 event. This is confirmed by the two-year averaged proportion of cultivated-type pixels affected by each drought (Table 2), which represents 32% for the 2007–2009 drought and below 30% for the 1998–2000 event.

5. Summary and conclusions

Droughts are relatively recurrent phenomena in the FC region, nevertheless prolonged and intense episodes such as the recent 2007–2009 drought can seriously affect the access to crops and food for a large population in this area. It is thought natural that a large percentage of the relatively sparse literature dealing with FC climate is devoted to a better characterization of droughts from a meteorological (e.g. Morid et al., 2006; Soltani et al., 2007), hydrological (e.g. Jones et al., 2008; Kitoh et al., 2008) or vegetation (e.g. Zaitchik et al., 2007; Bajgiran et al., 2008) perspective. Additionally, regional modelling studies tend to focus on dynamical capacity to reproduce dry/wet years dichotomies (Evans et al., 2004; Zaitchik et al., 2007), or improve statistical seasonal forecast of drought events (Soltani et al., 2007; Morid et al., 2007). Interestingly, the majority of these studies have looked in some detail at the last major prolonged drought that took place in the area, i.e. the 1998–2000 episode.

In this work we have made an effort to characterise in detail the outstanding strength of the recent prolonged 2007–2009 drought episode over the Middle East but with particular focus on most of the Fertile Crescent region. The study was broadly divided in two parts, with the first half aiming to provide an overview on the temporal and spatial amplitude of the event, as well as the atmospheric circulation anomalies leading to it, and the second half focusing on the impact of such unusual conditions on the vegetation dynamics and cereal production in the region.

After ranking all two-year drought events it becomes evident that this episode corresponds to the driest case for that area since 1940, albeit falling relatively close to the 1998–2000 event. Large sectors of Iraq received less than 40% of the average precipitation for those two years, although the suppression of rainfall was felt more acutely in the first hydrological year. An analysis on the associated large-scale atmospheric circulation provided some hints on the physical driving mechanisms responsible for such an unusual sequence of dry months. The wet months (ONDJFMAM) in both years were dominated by high pressures albeit with considerably different configurations in core winter (DJF) and transitional (ONAM) months. Naturally, these high pressure configurations inhibited synoptic activity entering FC from the eastern Mediterranean. Moreover, moisture fluxes over the affected area presented an easterly or north-easterly component, i.e. dry air masses were consistently advected from Iran and Russia. Finally, dry conditions also favoured low potential equivalent temperatures at 1000 hPa and a weaker-than-normal convective instability. It should be stressed that large-scale atmospheric circulation anomalies at the seasonal (or monthly) scales present a less clear picture than for other major droughts observed in middle latitude, such as Iberia (e.g. Garcia-Herrera et al., 2007). Nevertheless, seasonal composites highlight appreciable signatures and seasonal differences that are in agreement with an inhibition of the mechanisms conductive to precipitation. It has been shown that Mediterranean and Middle East precipitation regimes are partially influenced by the occurrence of El Niño and La Niña events (Mariotti et al., 2005). However, this influence is only significant during autumn, therefore failing to be incorporated as a useful predictor in statistical drought models developed for the area (e.g. Morid et al., 2007).

In the second part we looked at the evolution of monthly anomaly fields of NDVI, with the highest negative anomalies being found in April 2008 and affecting a region that corresponds to the northern sector of FC, being less intense over the eastern Mediterranean coastal mountainous area and the Tigris and Euphrates basin within Iraq. The evaluation of the accumulated number of months with negative NDVI values is particularly impressive during the first drought year (2007–2008) with pixels located over south-eastern Turkey, eastern Syria, northern Iraq and western

Iran presenting up to six months of persistently stressed vegetation between January and June 2008. The second drought year (2008–2009) presents smaller affected region restricted to northern Iraq, although still with up to five months of stressed vegetation. Finally we looked at the impacts on cereal (wheat and barley) production in the region. According to data provided by FAO, all three major cereal dependent countries in the area (Syria, Iraq and Iran) were deeply affected by this drought, particularly in the year 2008. The impact of drought is clearly visible in both wheat and barley productions, with significant economic losses in the affected countries.

The FC region is located at the eastern end of the Mediterranean basin, a region characterised by decreasing precipitation and river flow in the last few decades (Mariotti et al., 2008). The occurrence of the two strongest prolonged droughts in the last decade raises some concerns that this could become the norm, rather than the exception, in the future. In fact, according to the recent literature dealing with climate scenarios for the area, this tendency to dryness is expected to increase. According to the latest IPCC report (Christensen et al., 2007) most studies based on global and regional climate models suggest that the Mediterranean area will register a general trend towards less precipitation during the 21st century (e.g. Gibelin and Deque, 2003; Giorgi and Lionello, 2008). These results were also confirmed using the Earth-Machine Simulator, i.e. the highest resolution GCM available (Kitoh et al., 2008). The combined effects of this future precipitation decrease and the widely accepted future increment in the surface temperature on the Mediterranean (Christensen et al., 2007) will bear important changes in the region's hydrological water cycle.

The strong seasonal and inter-annual variability of vegetation in most semi-arid regions is a subject of particular interest due to the ecological and economic impacts. In particular, the high sensitivity of vegetation to climate forcing may result in rapid land use changes and high vulnerability to land degradation, as result of human action (Evans and Geerken, 2004). Over longer periods, small changes may have a considerable impact on the viability of agricultural and pastoral systems (deMenocal, 2001; Hole, 1994; Weiss and Bradley, 2001).

Acknowledgements

This study received support from the EU 6th Framework Program (CIRCE) contract number 036961 (GOCE) and from the Portuguese Science Foundation FCT through Project ENAC (PTDC/AAC-CLI/103567/2008). The NDVI dataset was kindly supplied by VITO database (http://free.vgt.vito.be). USDA/FAS/OGA and NASA Global Agriculture Monitoring (GLAM) Project. Lake and reservoir surface height variations from the USDA's Global Reservoir and Lake (GRLM) website at: http://www.pecad.fas.usda.gov/cropexplorer/global_reservoir/. Altimetric lake level time-series variations from the Topex/Poseidon, Jason-1, Jason-2/OSTM, and Geosat Follow-On (GFO) missions.

References

Bajgiran, P., Darvishsefat, A., Khalili, A., Makhdoum, M., 2008. Using AVHRR-based vegetation indices for drought monitoring in the northwest of Iran. J. Arid Environ. 72, 1086–1096.

Chen, J.L., Wilson, C.R., Tapley, B.D., Chambers, D.P., Pekker, T., 2001. Hydrological impacts on seasonal sea level change. Glob. Planet. Change 32, 25–32.

Christensen, J.H., Hewitson, B., Busuioc, A., Chen, A., Gao, X., Held, I., Jones, R., Kolli, R.K., Kwon, W.-T., Laprise, R., Magaña Rueda, V., Mearns, L., Menéndez, C.G., Räisänen, J., Rinke, A., Sarr, A., Whetton, P., 2007. Regional climate projections. In: Solomon, S., Qin, D., Manning, M., Chen, Z., Marquis, M., Averyt, K.B., Tignor, M., Miller, H.L. (Eds.), Climate Change 2007: The Physical Science Basis. Contribution of Working Group I to the Fourth Assessment Report of the Intergovernmental Panel on Climate Change. Cambridge University Press, Cambridge, United Kingdom/New York, NY, USA.

Cretaux, J.F., Kouraev, A., Berge-Nguyen, M., Cazenave, A., Papa, F., 2005. Satellite altimetry for monitoring lake level changes. In: Vogtmann, H., Dobretsov, N. (Eds.), Transboundary Water Resources: Strategies for Regional Security and Ecological Stability. Springer, Netherlands, pp. 141–146, doi:10.1007/1-4020-3082-7.

Dall'Olmo, G., Karnieli, A., 2002. Monitoring phenological cycles of desert ecosystems using NDVI and LST data derived from NOAA-AVHRR imagery. Int. J. Remote Sens. 23, 4055–4071.

deMenocal, P.B., 2001. Cultural responses to climate change during the Late Holocene. Science 292, 667–673.

Diouf, A., Lambin, E.F., 2001. Monitoring land-cover changes in semi-arid regions: remote sensing data and field observations in the Ferlo, Senegal. J. Arid Environ. 48, 129–148.

Eagleson, P., 2002. Ecohydrology. In: Darwinian Expression of Vegetation Form and Function. Cambridge University Press, Cambridge.

Evans, J.P., Geerken, R., 2004. Discrimination between climate and human-induced dryland degradation. J. Arid Environ. 57, 535–554.

Evans, J.P., Smith, R.B., Oglesby, R.J., 2004. Middle East climate simulation and dominant precipitation processes. Int. J. Climatol. 24, 1671–1694.

Freiwan, M., Kadioglu, M., 2008. Climate variability in Jordan. Int. J. Climatol. 28, 69–89.

Garcia-Herrera, R., Paredes, D., Trigo, R.M., Trigo, I.F., Hernández, H., Barriopedro, D., Mendes, M.T., 2007. The outstanding 2004–2005 drought in the Iberian Peninsula: the associated atmospheric circulation. J. Hydrometeor. 8, 483–498.

Gibelin, A.L., Deque, M., 2003. Anthropogenic climate change over the Mediterranean region simulated by a global variable resolution model. Clim. Dyn. 20, 237–339.

Giorgi, F., Lionello, P., 2008. Climate change projections for the Mediterranean region. Glob. Planet. Change 63, 90–104.

Gouveia, C., Trigo, R.M., DaCamara, C.C., 2009. Drought and vegetation stress monitoring in Portugal using satellite data. Nat. Hazards Earth Syst. Sci. 9, 185–195.

Hagolle, O., Lobo, A., Maisongrande, P., Duchemin, B., De Pereira, A., 2005. Quality assessment and improvement of SPOT/VEGETATION level temporally composited products of remotely sensed imagery by combination of VEGETATION 1 and 2 images. Remote Sens. Environ. 94, 172–186.

Holben, B.N., 1986. Characteristics of maximum-value composite images from temporal AVHRR data. Int. J. Remote Sens. 7, 1417–1434.

Hole, F., 1994. Environmental instabilities and urban origins. In: Chiefdoms and Early States in the Near East: the Organizational Dynamics of Complexity. Prehistory Press, pp. 121–151.

Iglesias, E., Garrido, A., Gomez-Ramos, A., 2003. Evaluation of drought management in irrigated areas. Agric. Econ. 29, 211–229.

Jones, C., Sultan, M., Yan, E., Milewski, A., Hussein, M., Aldousari, A., Alkaisy, S., Becker, R., 2008. Hydrologic impacts of engineering projects on the Tigris Euphrates system and its marshlands. J. Hydrol. 353, 59–75.

Kalnay, E., Kanamitsu, M., Kistler, R., Collins, W., Deaven, D., Gandin, L., Iredell, M., Saha, S., White, G., Wollen, J., Zhu, Y., Letman, A., Reynolds, R., Chelliah, M., Ebisuzaki, W., Higgins, W., Janowiak, J., Moo, K.C., Ropelewski, C., Wang, J., Jenne, R., Joseph, D., 1996. The NCEP/NCAR 40-year reanalysis project. Bull. Am. Meteorol. Soc. 77, 437–471.

Kitoh, A., Yatagai, A., Alpert, P., 2008. First super-high-resolution model projection that the ancient "Fertile Crescent" will disappear in this century. Hydrol. Res. Lett. 2, 1–4.

Kogan, F.N., 1995. Application of vegetation index and brightness temperature for drought detection. Adv. Space Res. 11, 91–100.

Kogan, F.N., 1997. Global drought watch from space. Bull. Am. Meteorol. Soc. 78, 621–636.

Kogan, F.N., 2000. Contribution of remote sensing to drought early warning. In: Wilhite, D.A., Sivakumar, V.K., Wood, D.A. (Eds.), Early Warning Systems for Drought Preparedness and Drought Management: Proceedings of an Expert Group Meeting. Lisbon, Portugal, September 5–7. WMO, Geneva, Switzerland, pp. 86–100.

Kogan, F.N., Usa, D.C., Stark, R., Gitelson, A., Jargalsaikhan, L., Dugarjav, C., 2004. Derivation of pasture biomass in Mongolia from AVHRR-based vegetation health indices. Int. J. Remote Sens. 25, 2889–2896.

Lucht, W.I., Colin Prentice, W.I., Myneni, R.B., Sitch, S., Friedlingstein, P., Cramer, W., Bousquet, P., Buermann, W., Smith, B., 2002. Climatic control of the high-latitude vegetation greening trend and Pinatubo effect. Science 296, 1687–1688.

Maisongrande, P., Duchemin, B., Dedieu, G., 2004. VEGETATION/SPOT—an operational mission for the earth monitoring: presentation of new standard products. Int. J. Remote Sens. 25, 9–14.

Mariotti, A., Ballabrera-Poy, J., Zeng, N., 2005. Tropical influence on Euro-Asian autumn rainfall. Climate Dyn. 24, 511–521, doi:10.1007/s00382-004r-r0498-6.

Mariotti, A., Zeng, N., Yoon, J., Artale, V., Navarra, A., Alpert, P., Li, L.Z.X., 2008. Mediterranean water cycle changes: transition to drier 21st century conditions in observations and CMIP3 simulations. Environ. Res. Lett. 3, 044001, doi:10.1088/1748-9326/3/4/044001.

McVicar, T.R., Jupp, D.L.B., 1999. Estimating one-time-of-day meteorological data from standard daily data as inputs to thermal remote sensing based energy balance models. Agric. Forest Meteor. 96, 219–238.

McVicar, T.R., Jupp, D.L.B., 2002. Using covariates to spatially interpolate moisture availability in the Murray-Darling Basin: a novel use of remotely sensed data. Remote Sens. Environ. 79, 199–212.

Morales, A., Olcina, J., Rico, A.M., 2000. Diferentes percepciones de la sequía en España: adaptación, catastrofismo e intentos de corrección (The different perceptions about droughts in Spain: adaptations and correction systems). Investigaciones Geográficas 23, 5–46 (in Spanish).

Morid, S., Smakhtin, V., Moghaddasi, M., 2006. Comparison of seven meteorological indices for drought monitoring in Iran. Int. J. Climatol. 26, 971–985.
Morid, S., Smakhtin, V., Bagherzadeh, K., 2007. Drought forecasting using artificial neural networks and time series of drought indices. Int. J. Climatol. 27, 2103–2111.
Nemani, R.R., Charles, D., Keeling, C.D., Hashimoto, H., Jolly, W.M., Piper, S.C., Tucker, C.J., Myneni, R.B., Running, S.W., 2003. Climate-driven increases in global terrestrial net primary production from 1982 to 1999. Science 300, 1560–1563.
Nicholson, S.E., Tucker, C.J., Ba, M.B., 1998. Desertification, drought and surface vegetation: an example from the West African Sahel. Bull. Am. Meteorol. Soc. 79, 815–829.
Rodríguez-Iturbe, I., Porporato, A., 2004. Ecohydrology of water-controlled ecosystems. Cambridge.
Rudolf, B., Meyer-Christoffer, A., 2005. Hydrometeorological conditions during the extremely dry year 2003 in the long-term and European context. In: Annual Bulletin on the Climate in WMO Region VI—2003, pp. 87–93.
Rudolf, B., Schneider, U., 2005. Calculation of gridded precipitation data for the global land-surface using in-situ gauge observations. In: Proceedings of the 2nd Workshop of the International Precipitation Working Group IPWG, EUMETSAT, Monterey October 2004, ISBN: 92-9110-070-6, ISBN: 1727-432X, 231-247.
Schmidt, H., Karnieli, A., 2000. Remote sensing of the seasonal variability of vegetation in a semi-arid environment. J. Arid Environ. 45, 43–59.
Shean, M., 2008a. Iran: 2008/09 wheat production declines due to drought. United States Department of Agriculture, Foreign Agricultural Service. May 9. Accessed 30.05.08.
Shean, M., 2008b. Iraq: drought reduces 2008/09 winter grain production. United States Department of Agriculture, Foreign Agricultural Service. May 9. Accessed 30.05.08.
Shean, M., 2008c. Syria: wheat production in 2008–09 declines owing to season-long drought. United States Department of Agriculture, Foreign Agricultural Service. May 9. Accessed 30.05.08.
Soltani, S., Modarres, R., Eslamian, S.S., 2007. The use of time series modeling for the determination of rainfall climates of Iran. Int. J. Climatol. 27, 819–829.
Trenberth, K.E., Guillemot, C.J., 1995. Evaluation of the global atmospheric moisture budget as seen from analyses. J. Climate 8, 2255–2280.
Trigo, I.F., Davies, T.D., Bigg, G.R., 1999. Objective climatology of cyclones in the Mediterranean region. J. Climate 12, 1684–1696.
Vicente-Serrano, S.M., 2006. Spatial and temporal analysis of droughts in the Iberian Peninsula (1910–2000). Hydrol. Sci. J. 51, 83–97.
Vicente-Serrano, S.M., 2007. Evaluating the impact of drought using remote sensing in a Mediterranean, semi-arid region. Nat. Hazards 40, 173–208, doi:10.1007/s11069-006-0009-7.
Vicente-Serrano, S.M., Heredia-Laclaustra, A., 2004. NAO influence on NDVI trends in the Iberian Peninsula (1982–2000). Int. J. Remote Sens. 25, 2871–2879.
Weiss, J.L., Gutzler, D.S., Coonrod, J.E.A., Dahm, C.N., 2004. Long-term vegetation monitoring with NDVI in a diverse semi-arid setting, central New Mexico, USA. J. Arid Environ. 58, 249–272.
Weiss, E., Marsh, S.E., Pfirman, E.S., 2001. Application of NOAA-AVHRR NDVI time-series data to assess changes in Saudi Arabia's rangelands. Int. J. Remote Sens. 22, 1005–1027.
Weiss, H., Bradley, R.S., 2001. What drives societal collapse? Science 291, 609–610.
Wilhite, D.A., 1993. Understanding the phenomenon of drought. Hydro-Review 12, 136–148.
Zaitchik, B.F., Evans, J.P., Geerken, R.A., Smith, R.B., 2007. Climate and vegetation in the Middle East: interannual variability and drought feedbacks. J. Climate 20, 3924–3941.
Zhou, L., Tucker, C.J., Kaufmann, R.K., Slayback, D., Shabanov, N., Myneni, R.B., 2001. Variations in northern vegetation activity inferred from satellite data of vegetation index during 1981 to 1999. J. Geophys. Res. 106, 20069–20083.